Physics and Imaging in Radiation Oncology 27 (2023) 100472

Contents lists available at ScienceDirect

Physics and Imaging in Radiation Oncology

journal homepage: www.sciencedirect.com/journal/physics-and-imaging-in-radiation-oncology

Original Research Article

# Cone beam computed tomography image guidance within a magnetic resonance imaging-only planning workflow

Laura M. O'Connor [a,b,*], Alesha Quinn [a], Samuel Denley [a], Lucy Leigh [c], Jarad Martin [a], Jason A Dowling [d], Kate Skehan [a], Helen Warren-Forward [b], Peter B. Greer [a,e]

[a] Department of Radiation Oncology, Calvary Mater Hospital, Edith Street, Waratah, Newcastle, NSW 2298, Australia
[b] School of Health Sciences, University of Newcastle, University Drive, Newcastle, NSW 2308, Australia
[c] Hunter Medical Research Institute, Lot 1 Kookaburra Ct, New Lambton Heights, NSW 2305, Australia
[d] Australian E-Health Research Centre, Commonwealth Scientific and Industrial Research Organisation (CSIRO), Bowen Bridge Rd, Herston, QLD 4029, Australia
[e] School of Information and Physical Sciences, University of Newcastle, University Drive, Newcastle, NSW 2308, Australia

ARTICLE INFO

*Keywords:*
Radiotherapy
Image-guided radiation therapy
MRI-only radiotherapy planning
Cone Beam Computed Tomography
MRI guided radiation therapy
Magnetic resonance imaging

ABSTRACT

*Background and purpose:* Magnetic Resonance Imaging (MRI)-only planning workflows offer many advantages but raises challenges regarding image guidance. The study aimed to assess the viability of MRI to Cone Beam Computed Tomography (CBCT) based image guidance for MRI-only planning treatment workflows.
*Materials and methods:* An MRI matching training package was developed. Ten radiation therapists, with a range of clinical image guidance experience and experience with MRI, completed the training package prior to matching assessment. The matching assessment was performed on four match regions: prostate gold seed, prostate soft tissue, rectum/anal canal and gynaecological. Each match region consisted of five patients, with three CBCTs per patient, resulting in fifteen CBCTs for each match region. The ten radiation therapists performed the CBCT image matching to CT and to MRI for all regions and recorded the match values.
*Results:* The median inter-observer variation for MRI-CBCT matching and CT-CBCT matching for all regions were within 2 mm and 1 degree. There was no statistically significant association in the inter-observer variation in mean match values and radiation therapist image guidance experience levels. There was no statistically significant association in inter-observer variation in mean match values for MRI experience levels for prostate soft tissue and gynaecological match regions, while there was a statistically significant difference for prostate gold seed and rectum match regions.
*Conclusion:* The results of this study support the concept that with focussed training, an MRI to CBCT image guidance approach can be successfully implemented in a clinical planning workflow.

## 1. Introduction

Magnetic Resonance Imaging (MRI) has advanced in its utilisation for radiation oncology, with much of the target region and organ at risk (OAR) contouring performed on a planning MRI, acquired in the treatment position, and transferred across to a computed tomography (CT) for treatment planning [1,2]. However, this transfer across has the potential to introduce systematic errors, which arise from errors in the initial registration process between modalities [3,4]. Therefore, MRI-only radiation therapy planning is becoming an increasingly popular concept, superseding the conventional use of a simulation CT for treatment planning. To facilitate an MRI-only planning workflow, an electron/mass density map is created from the MRI, termed a synthetic CT (sCT), to enable accurate treatment planning dose calculation [5,6].

In the radiation therapy workflow, the treatment planning data set is also utilised for daily online image guidance, to allow for accurate localisation for treatment delivery. Several studies have assessed various methods for sCT generation and the dosimetric outcomes, however in the absence of a planning CT for MRI-only workflows, image guidance solutions also need to be evaluated [6–10]. The treatment planning and

*Abbreviations:* CBCT, Cone Beam Computed Tomography; DRR, Digitally reconstructed radiograph; GTV, Gross Tumour Volumel; PTV, Planning Target volume; sCT, synthetic Computed Tomography.

* Corresponding author at: Department of Radiation Oncology, Calvary Mater Hospital, 20 Edith St, Waratah, Newcastle, NSW 2298, Australia.
*E-mail address:* Laura.OConnor@calvarymater.org.au (L.M. O'Connor).

https://doi.org/10.1016/j.phro.2023.100472
Received 15 May 2023; Received in revised form 6 July 2023; Accepted 6 July 2023
Available online 8 July 2023

delivery systems are designed so that current departmental procedures use the sCT as a reference image for image guidance on treatment. However, given the sCT is not a true anatomical image, but a synthetically generated density map for dose calculation, it should ideally not be used for image guidance. However effective the sCT generation method is in creating a realistic sCT from the MRI, there are still regions for anatomical error in the sCT generation process [6,11]. These errors are systematic and are transferred to the treatment delivery when used for image guidance [12], while some sCT generation processes do not create sufficient anatomical information for image guidance [9]. Therefore, it would be pertinent to determine if the MRI scan that the sCT is generated from, could be used for Cone-Beam CT (CBCT) image guidance, as using an anatomical image such as the MRI as the reference image, would provide greater soft tissue contrast and potentially matching accuracy. This would allow for a greater utility of MRI-only planning for all pelvic treatment sites. In addition, when the planning MRI is treated as the primary contouring data set and the CT for dose calculation within a traditional treatment planning workflow, then utilising an MRI-CBCT image matching workflow has the potential to reduce the systematic errors associated with image fusion and target region translation between images in the treatment planning process.

As current practice is to use CT to CBCT as image guidance, it should be determined if the substitution of MRI to CBCT for image guidance affects the accuracy of the image matching. There is limited work around MRI to CBCT image guidance, with publications mostly focusing on sCT-CBCT image guidance [13–16]. Two studies, which focused on MRI-CBCT image guidance, have assessed the soft tissue match accuracy for prostate treatments, while another study focused on anal canal and rectum, utilising only one matcher with automatic registration [17–19]. While the results of these studies appear promising, additional work on this topic has identified that a training package reduces the inter-observer variability in MRI-CBCT matching, to align with the variability of CT-CBCT matching values [20].

The aim of this study was to retrospectively investigate if the substitution of MRI to CBCT for image guidance affects the accuracy of the image matching for a range of pelvic treatment sites.

## 2. Materials and methods

Ethics approval was granted through Hunter New England ethics committee (ref:17/06/21/3.02 & 2019/ETH09769) and twenty patients receiving radiation treatment to the pelvic region gave informed consent. Patients were separated into four cohorts for the study based on treatment regions and matching objectives: prostate gold seeds, prostate soft tissue, rectum/anal canal and gynaecological.

Planning CT and MRI were acquired in the treatment position, utilising positioning tattoos for similar alignment of patients between the scanning modalities. Planning CTs were acquired on a SOMATOM Confidence CT scanner (Siemens Healthineers; Erlangen, Germany). Planning MRIs were performed on a MAGNETOM Skyra 3 T MRI scanner (Siemens Healthineers; Erlangen, Germany), typically within 15 min after the CT scan. The MRI scanner was equipped with a Qfix flat couch (Qfix; Pennsylvania USA) and DORADOnova MR 3 T external laser bridge (LAP; Luneburg, Germany). An 18-channel body coil was positioned in a Qfix INSIGHT MR Body coil holder over the pelvic region and a 32-channel spine coil was utilised under the flat couch top. A standard T1 Volume Interpolated Breath-hold Examination (VIBE) Dixon MRI was acquired for the purpose of this study.

Ten radiation therapists participated in the study matching. Radiation therapist image guidance experience was classified into two categories of: base grade image guidance and stereotactic specialised image guidance. MRI experience levels were self-reported by all participants (Supplement A).

### 2.1. Training package

An MRI image matching training package was developed by two MRI trained radiation therapists, based on a previously successful training model [20]. The training package comprised of basic MRI tissue weightings, MRI anatomy of the pelvis in males and females, identification of key anatomical features on T1 and T2-weighted MRI, and the rationale behind MRI matching for MRI-only planning workflows. This was followed by three trial matches between an MRI and CBCT for pelvic patients, using both bony registration and soft tissue matching. All ten radiation therapists completed the training package prior to matching assessment, regardless of previous experience.

### 2.2. Image matching

All data sets were anonymised, and the T1 VIBE Dixon MRI scan was rigidly registered to the CT using automatic rigid registration in the Eclipse 15.6 (Varian Medical Systems Inc., Palo Alto, CA, USA) registration module. The gross tumour volume (GTV), clinical target volume (CTV) and planning target volume (PTV) were all transferred to the T1 VIBE Dixon MRI scan to assist in clinical decision making. The OARs and gold seed fiducial markers (prostate gold seed cohort only) were re-contoured on the T1 VIBE Dixon MRI scan. The identification of the gold seed fiducial markers on the MRI was validated against the planning CT scan.

Image matching was performed in the ARIA (Varian Medial Systems Inc., Palo Alto, CA, USA) offline review module. Prostate gold seed overlay structures were utilised on the CT and MRI and matched to the visible seeds on CBCT, while prostate soft tissue image matching was a match to the prostate, in the absence of gold seed fiducials. Rectum/anal canal image matching utilised an automatic bone registration, and manual adjustment if the GTV was outside the PTV volume, dependent on rectal volume. Gynaecological image matching was an initial automatic bone registration, followed by a manual primary match to the vaginal vault and/or endometrial region, dependent on daily rectal and bladder filling. The workflow is outlined in Supplement B.

For each match region there were three CBCT scans (start, middle and end of treatment course time points) per patient with five patients per region, giving fifteen images per treatment region. The ten radiation therapists performed image matching for each image, resulting in 150 matches per region. The CBCT datasets used for the matches were all reset to the treatment acquisition position in offline review. CBCT matchings were initially performed to CT, a minimum one-week interval elapsed before matches to the T1 MRI were subsequently performed. The final match positions (FMP) were recorded for each match, representing the difference between the therapist's study match position and the previously performed clinical match (designated as 0 position by the matching software). However, it should be noted that a value of zero does not designate a perfect match (gold-standard is not known), just that the study match has closely reproduced the clinical match.

Linear mixed effects modes were utilised to estimate the mean match positions and adjust the variance for repeated measures for CT-CBCT and MRI-CBCT respectively, for each match region. Random intercepts for patient and radiation therapist to account for the repeated images per patient, and the repeated radiation therapists measuring each image.

For each match region ($k$) the overall mean FMP was calculated ($\overline{x}_k$) for each direction. This measure assesses if there is any overall bias in the matching for the different modalities. The linear mixed effects models were then adjusted for radiation therapist experience and MRI experience respectively, to determine whether there was any difference in the matching between the different experience levels. The FMP recorded for therapist $j$ for image $i$ is denoted ($x_{ij}$). The mean FMP, for image $i$ across a total of $J$ therapists is denoted $\overline{x}_i = \sum_{j=1}^{J} x_{ij}/J$. These results were assessed using the Bland-Altman plot.

The inter-observer variation (IOV) for each image was calculated (as

the standard deviation of the ten radiation therapist FMP's) per scan $\sigma_i$. For each region and direction of measurement the median IOV and Inter-Quartile Range (IQR) were determined, for CT-CBCT and MRI-CBCT respectively [21].

## 3. Results

The mean match positions $\bar{x}_k$ across all directions (Table 1) were $\leq$0.05 mm and <0.5° for all matching regions in MRI-CBCT matching and <0.1 mm and <0.3° across all matching regions in CT-CBCT matching. There was no statistically significant difference ($p > 0.05$) in the mean match position associated with radiation therapist image guidance experience. There was no statistically significant difference ($p > 0.05$) in the mean match position associated with previous MRI experience for prostate soft tissue or gynaecological matching. There was a statistically significant difference between groups in terms of mean match position for MRI experience for CT and MRI rotational in prostate gold seed (CT $p = 0.02$, MRI $p < 0.01$) and statistically significant difference between groups in terms of mean match position for MRI experience for CT lateral ($p < 0.01$) and MRI longitudinal ($p < 0.01$) in rectum CBCT matching.

Fig. 1 shows as an example the prostate soft tissue Bland-Altman plots of inter-observer variability in each direction for CT-CBCT and MRI-CBCT match positions. For each CBCT registration, the difference between each recorded registration position and its corresponding mean image registration position ($\bar{x}_{ij}$ - $x_i$) was plotted against the overall mean registration position $x_i$ [22]. The limits of agreement for all regions were within 0.5 mm for cartesian direction and 1 mm for rotations, while the difference in limits of agreement between the CT and MRI were within 0.2 mm and 1 degree for all areas. The plots for prostate gold seed (Supplement C), rectum (Supplement D) and gynaecological (Supplement E) are included in the supplementary material.

Table 2 shows the IOV for each region and direction. The median IOV for the MRI-CBCT and CT-CBCT were<0.25 mm and 1 degree. The median IOV was consistently higher for MRI-CBCT than CT-CBCT for all areas and match directions. The greatest difference in median values was observed in the IOV for rotation for the MRI-CBCT compared to the CT-CBCT. This is particularly evident for the prostate gold seed matching, with a median (IQR) IOV of 0.86° (0.51°, 1.03°) in the MRI-CBCT matching compared to the CT-CBCT median of 0.30° (0.07°, 0.48°).

## 4. Discussion

This study evaluated the use of MRI to CBCT for image guidance of a range of pelvic treatment sites and image matching objectives. This is the first study, to the authors knowledge, which investigates the use of MRI-CBCT image guidance for prostate soft tissue, prostate gold-seed, rectum and gynaecological collectively. While the image matching processes and aims are different between the sites, the results in matching variability amongst the cohort of radiation therapists were similar, with a median IOV in MRI-CBCT matching of $\leq$ 2 mm. The greatest variability was observed in the rotational IOV for each site, with the median value of 0.86° being greatest in the prostate gold-seed MRI-CBCT cohort, this may be due to the difficulty in identifying the gold seeds on the MRI and may need more research in this area. Given the minimal dosimetric impact of such a small rotation, reassuringly this would not have any significant clinical consequences [23].

On average, the inter-observer variability in the MRI-CBCT matching was higher than the variability in the CT-CBCT matching, however the difference in the variability median values is<1 mm for all groups. Therefore, for this cohort of patients, with PTV margins > 5 mm on the CTV, the minimal difference between the variability can be considered not clinically significant. While the translational measurements are simpler to relate directly to PTV margins, it is difficult to ascertain the effect of rotation on target location and PTV margins.

A large field of view T1 VIBE Dixon MRI was utilised in this study for image matching, due to other acquired MRI sequences having insufficient field of view. The T1-weighted Dixon is a commonly utilised sequence for sCT generation [6,10,16], however T2-weighted sequences used for sCT generation have also been successfully utilised for CBCT image guidance [19]. The MRI sequences used for synthetic CT creation may be considered most appropriate for this application if it meets the requirements of a large field of view and high geometric fidelity over the treatment region.

The findings correlate with previous studies in the area, such as Wyatt et al., who investigated MRI-CBCT prostate soft tissue matching [19]. Wyatt et al reported a similar mean inter-observe error to this study, and all IOV within 3.3 mm [19]. Other studies have assessed MRI-CBCT matching using automatic registration algorithms. Edmund et al. assessed automatic registration for prostate with a resulting 2 mm difference amongst the matching cohort, while Bird et al., assessed a single observer automatic registration for rectal and anal canal regions [17,24]. Bird et al., reported a < 1 mm difference and < 0.4° in automatic registration differences [17]. While the reported difference was lower for Bird et al., than in this study, the use of automatic registration is not necessarily reflective of clinical practice, as clinical decisions and adjustments to the image matching need to be made for anatomical changes daily, therefore, these studies do not take into account the differences imparted from MRI image interpretation in image guidance.

While this study investigated the inter-observer variability of a single radiation therapist performing each of the image matching, this is not necessarily reflective of clinical practice, in which ordinarily a team of at

**Table 1**
Mean match position ($\bar{x}_k$) for CT-CBCT, and MRI-CBCT image matching for each region and direction (lateral, longitudinal, and vertical (mm), rotational (°)).

| | | *MRI-CBCT* | | | *CT-CBCT* | | |
|---|---|---|---|---|---|---|---|
| *Variable* | | *Mean* | *Standard error* | *p-value* | *Mean* | *Standard error* | *p-value* |
| Prostate soft tissue | Lateral (mm) | 0.02 | 0.01 | 0.01 | 0.02 | 0.01 | 0.02 |
| | Longitudinal (mm) | −0.05 | 0.02 | 0.02 | −0.05 | 0.02 | 0.01 |
| | Vertical (mm) | 0.05 | 0.22 | 0.04 | 0.02 | 0.02 | 0.01 |
| | Rotation (°) | −0.24 | 0.07 | <0.01 | −0.28 | 0.07 | <0.01 |
| Prostate gold seed | Lateral (mm) | 0.03 | 0.01 | 0.02 | 0.03 | 0.01 | <0.01 |
| | Longitudinal (mm) | −0.04 | 0.01 | <0.01 | −0.03 | 0.01 | 0.04 |
| | Vertical (mm) | 0.00 | 0.01 | <0.01 | −0.01 | 0.01 | 0.02 |
| | Rotation (°) | 0.42 | 0.09 | <0.01 | 0.14 | 0.03 | <0.01 |
| Rectum | Lateral (mm) | 0.02 | 0.01 | 0.04 | −0.08 | 0.01 | 0.10 |
| | Longitudinal (mm) | −0.04 | 0.02 | <0.01 | −0.02 | 0.01 | 0.25 |
| | Vertical (mm) | 0.04 | 0.02 | 0.01 | 0.08 | 0.01 | <0.01 |
| | Rotation (°) | 0.00 | 0.04 | 0.34 | −0.06 | 0.03 | 0.10 |
| Gynaecological | Lateral (mm) | −0.01 | 0.01 | 0.11 | −0.02 | 0.01 | 0.01 |
| | Longitudinal (mm) | 0.05 | 0.02 | <0.01 | 0.02 | 0.01 | 0.09 |
| | Vertical (mm) | 0.04 | 0.02 | 0.04 | 0.01 | 0.02 | 0.06 |
| | Rotation (°) | −0.12 | 0.12 | 0.34 | 0.03 | 0.13 | 0.82 |

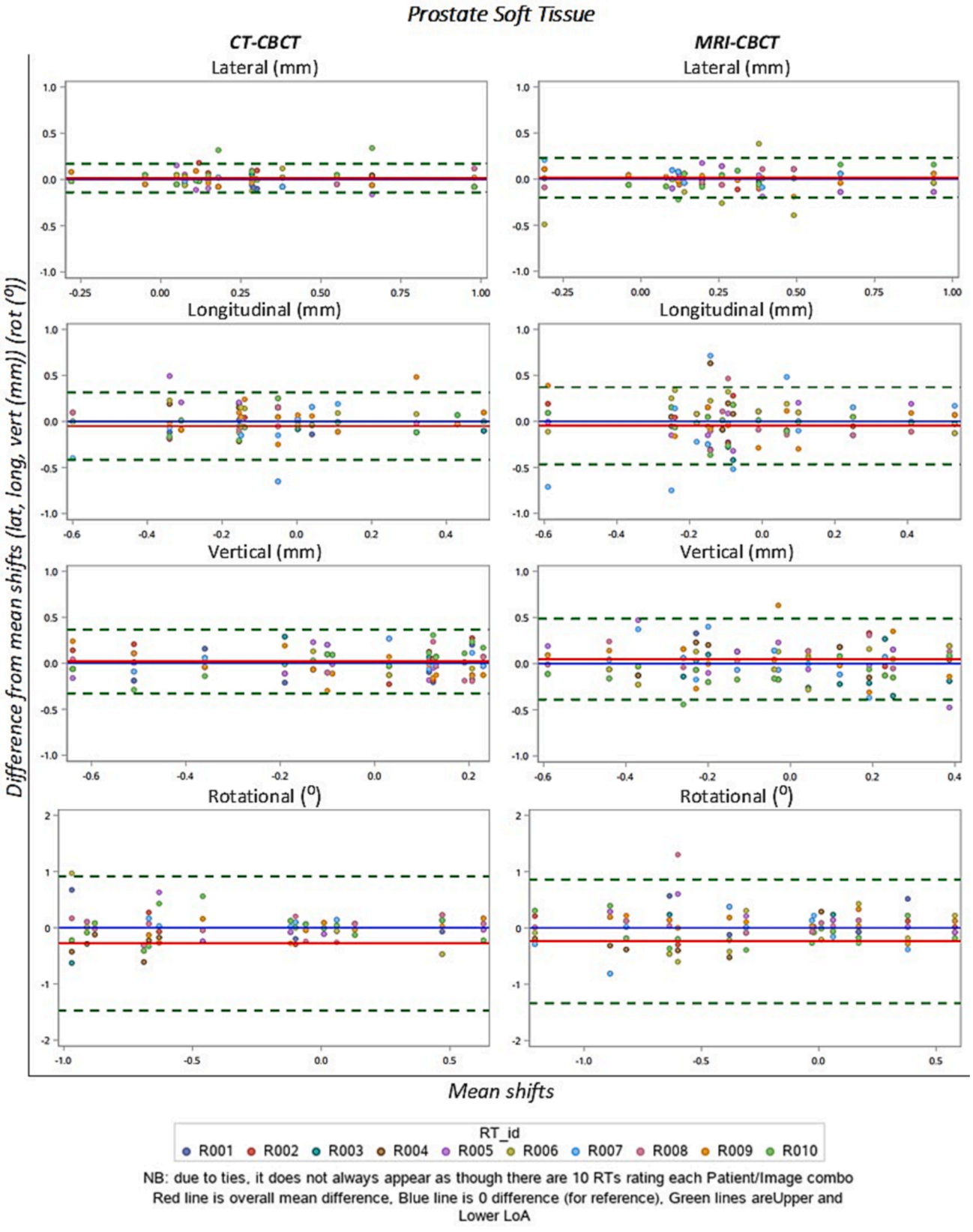


**Fig. 1.** Bland-Altman plots of the difference in match for each observer by the mean of all observers (for each CBCT scan that is registered) for prostate soft tissue. Each coloured dot represents a single radiation therapist each. Note that due to ties, it does not always appear as though there are 10 dots for each site. The red line is the overall mean difference, blue line is the 0 difference (for reference) and the green lines are the upper and lower limits of agreement. (For interpretation of the references to colour in this figure legend, the reader is referred to the web version of this article.)

**Table 2**
IOV (Median and IQR) for each region in each direction (lateral, longitudinal, and vertical (mm), rotational (°)).

| | | *MRI-CBCT* | | *CT-CBCT* | |
|---|---|---|---|---|---|
| *Variable* | | *Median* | *IQR* | *Median* | *IQR* |
| Prostate soft tissue | Lateral (mm) | 0.08 | (0.07,0.13) | 0.06 | (0.05,0.08) |
| | Longitudinal (mm) | 0.17 | (0.12,0.27) | 0.11 | (0.08,0.15) |
| | Vertical (mm) | 0.19 | (0.15,0.22) | 0.12 | (0.10,0.15) |
| | Rotation (°) | 0.21 | (0.19,0.33) | 0.15 | (0.12,0.29) |
| Prostate gold seed | Lateral (mm) | 0.07 | (0.05,0.08) | 0.05 | (0.03,0.08) |
| | Longitudinal (mm) | 0.08 | (0.06,0.12) | 0.08 | (0.07,0.11) |
| | Vertical (mm) | 0.06 | (0.05,0.07) | 0.06 | (0.05,0.07) |
| | Rotation (°) | 0.86 | (0.51,1.03) | 0.30 | (0.07,0.48) |
| Rectum | Lateral (mm) | 0.07 | (0.06,0.09) | 0.07 | (0.06,0.11) |
| | Longitudinal (mm) | 0.12 | (0.07,0.13) | 0.08 | (0.06,0.11) |
| | Vertical (mm) | 0.14 | (0.07,0.17) | 0.13 | (0.08,0.15) |
| | Rotation (°) | 0.25 | (0.07,0.34) | 0.21 | (0.10,0.32) |
| Gynaecological | Lateral (mm) | 0.08 | (0.05,0.10) | 0.07 | (0.05,0.11) |
| | Longitudinal (mm) | 0.13 | (0.10,0.18) | 0.12 | (0.10,0.13) |
| | Vertical (mm) | 0.20 | (0.17,0.25) | 0.14 | (0.11,0.19) |
| | Rotation (°) | 0.35 | (0.19,0.49) | 0.27 | (0.12,0.48) |

least two radiation therapists perform the daily image matching. Therefore, the combined input from two radiation therapists, may invariably reduce the outliers of the inter-observer variability results.

Brooks et al. indicated that the application of a training package resulted in a lower inter-observer variability in MRI-CBCT matching than without [20]. Due to the lack of pre-post testing in this study, it is difficult to determine in this study if the training package similarly affected the inter-observer variability in the MRI-CBCT matching. The results showed no significant difference in the results based on therapist image guidance experience, but there were mixed results based on MRI experience. There were no observed differences in the results in relation to MRI experience for prostate soft tissue or gynaecological regions. There was a positive correlation in the results in terms of MRI experience for both CT-CBCT and MRI-CBCT image matching for prostate gold-seed and rectum image matching. Given CT-CBCT was equally affected by MRI experience, the differences may not be related to MRI image interpretation, but rather could be attributed to some other undetermined factor, such as greater experience or specialisation in general image interpretation.

MRI is still a new and emerging technology in radiation therapy, with radiation therapists having greater experience in CT image guidance than MRI. It would be useful to repeat this study after a significant period has elapsed after a clinical roll out of MRI-CBCT image guidance. It is possible that the daily application of MRI-CBCT image guidance would increase the experience levels of radiation therapists in MRI image interpretation and bring the results further in-line with the variability in CT-CBCT.

This study was limited to an older data set, resulting in the inability to apply pitch and roll to the image matches. This is not reflective of current clinical practice which allows for six-degrees of movement for image matching. The lack of pitch and roll application in this data set could have introduced some inevitable variations between matchers due to the need to make compromises when the patient positioning does not align. Although efforts were made to replicate the CT simulation position in MRI, variations could also have been introduced due to different time points between modalities. Anatomical variations between scans such as bladder filling, bowel gas location and hip rotation/angulation could have affected the ability of matching to the MRI scan compared to the CT scan. This may have been reduced in this study if the MRI were deformably registered to the CT prior to CBCT image matching and could be applied to future studies in this field. This could be one explanation for the greater rotational variation in the prostate gold-seed cohort with greater bladder filling possibly contribution to greater rotational differences in the MRI. Also, the additional rotational information provided by the gold seeds when compared to the soft tissue on CBCT, could have also provided a reason for greater rotational application in this cohort.

The results of this study are not only applicable to an MRI-only planning workflow but can also be relevant to a traditional CT based planning workflow, in which there may be a prospective greater reliance on a planning MRI for the target and OAR contouring, thereby potentially reducing the systematic errors associated with the image fusion process in planning.

Currently the linear accelerator software does not facilitate the use of MRI scans or supplementary scans for daily image guidance. As such, a work around is required to accommodate this, by re-labelling the MRI DICOM tag as a CT, and to transfer the treatment plan from the sCT to the co-registered MRI, to allow MRI based daily image guidance [19]. This may delay the uptake of MRI-CBCT image guidance in an MRI-only treatment planning workflow. However, this study supports the adoption of MRI image guidance within the MRI-only planning workflow, particularly once the vendor treatment software is updated for MRI based clinical practice.

## CRediT authorship contribution statement

**Laura M. O'Connor:** Conceptualization, Methodology, Investigation, Writing – original draft, Project administration. **Alesha Quinn:** Investigation, Methodology. **Samuel Denley:** Investigation, Methodology. **Lucy Leigh:** Formal analysis, Software, Writing – review & editing. **Jarad Martin:** Writing – review & editing. **Jason A Dowling:** Conceptualization, Writing – review & editing. **Kate Skehan:** Resources, Conceptualization, Writing – review & editing. **Helen Warren-Forward:** Conceptualization, Writing – review & editing. **Peter B. Greer:** Conceptualization, Methodology, Writing – review & editing, Supervision.

## Declaration of Competing Interest

The authors declare that they have no known competing financial interests or personal relationships that could have appeared to influence the work reported in this paper.

## Acknowledgements

The authors wish to thank Ashlee Campbell, Christine Hudson, Jo Higgins, Joel Parker, Janine Robertson, Megan Farrell, Matt Richardson, Amy Zerafa, Alicia Hoye, Joerg Lehmann and Kenway Yeoh, for their time and support provided to this study

## Appendix A. Supplementary data

Supplementary data to this article can be found online at https://doi.org/10.1016/j.phro.2023.100472.

## References


[1] Salembier C, Villeirs G, De Bari B, Hoskin P, Pieters BR, Van Vulpen M, et al. ESTRO ACROP consensus guideline on CT- and MRI-based target volume delineation for primary radiation therapy of localized prostate cancer. Radiother Oncol 2018;127:49–61. https://doi.org/10.1016/j.radonc.2018.01.014.

[2] Dirix P, Haustermans K, Vandecaveye V. The value of magnetic resonance imaging for radiotherapy planning. Semin Radiat Oncol 2014;24:151–9. https://doi.org/10.1088/0031-9155/59/21/R349.

[3] Persson E, Emin S, Scherman J, Jamtheim Gustafsson C, Brynolfsson P, Ceberg S, et al. Investigation of the clinical inter-observer bias in prostate fiducial marker image registration between CT and MR images. Radiat Oncol 2021;16:150. https://doi.org/10.1088/1361-6560/aa5fa2.

[4] Nyholm T, Nyberg M, Karlsson MG, Karlsson M. Systematisation of spatial uncertainties for comparison between a MR and a CT-based radiotherapy workflow for prostate treatments. Radiat Oncol 2009;4:54. https://doi.org/10.1088/1361-6560/aa5fa2.

[5] Dowling J, O'Connor L, Acosta O, Raniga P, Crevoisierd R, Nunes JC, et al. Image synthesis for MRI-only radiotherapy treatment planning. In: Burgos N, Svoboda D, editors. Biomedical Image Synthesis and Simulation: Methods and Applications. Academic Press; 2022. https://doi.org/10.1016/B978-0-12-824349-7.00027-X.

[6] Bird D, Henry AM, Sebag-Montefiore D, Buckley DL, Al-Qaisieh B, Speight R. A Systematic Review of the Clinical Implementation of Pelvic Magnetic Resonance Imaging-Only Planning for External Beam Radiation Therapy. Int J Radiat Oncol Biol Phys 2019;105:479–92. https://doi.org/10.1016/j.ijrobp.2019.06.2530.

[7] Johnstone E, Wyatt JJ, Henry AM, Short SC, Sebag-Montefiore D, Murray L, et al. Systematic Review of Synthetic Computed Tomography Generation Methodologies for Use in Magnetic Resonance Imaging-Only Radiation Therapy. Int J Radiat Oncol Biol Phys 2018;100:199–217. https://doi.org/10.1016/j.ijrobp.2017.08.043.

[8] Wyatt JJ, Pearson RA, Walker CP, Brooks RL, Pilling K, McCallum HM. Cone beam computed tomography for dose calculation quality assurance for magnetic resonance-only radiotherapy. Phys Imaging Radiat Oncol 2021;17:71–6. https://doi.org/10.1016/j.phro.2021.01.005.

[9] O'Connor LM, Choi JH, Dowling JA, Warren-Forward H, Martin J, Greer PB. Comparison of Synthetic Computed Tomography Generation Methods, Incorporating Male and Female Anatomical Differences, for Magnetic Resonance Imaging-Only Definitive Pelvic Radiotherapy. Front Oncol 2022;12:822687. https://doi.org/10.3389/fonc.2022.822687.

[10] O'Connor LM, Skehan K, Choi JH, Simpson J, Martin J, Warren-Forward H, et al. Optimisation and validation of an integrated magnetic resonance imaging-only radiotherapy planning solution. Phys Imaging Radiat Oncol 2021;20:34–9. https://doi.org/10.1016/j.phro.2021.10.001.

[11] O'Connor LM, Dowling JA, Choi JH, Martin J, Warren-Forward H, Richardson H, et al. Validation of an MRI-only planning workflow for definitive pelvic radiotherapy. Radiat Oncol 2022;17:55. https://doi.org/10.1186/s13014-022-02023-4.

[12] Tyyger M, Nix M, Al-Qaisieh B, Teo MT, Speight R. Identification and separation of rigid image registration error sources, demonstrated for MRI-only image guided radiotherapy. Biomed Phys Eng Express 2020;6:035032. https://doi.org/10.1088/2057-1976/ab81ad.

[13] Kemppainen R, Suilamo S, Ranta I, Pesola M, Halkola A, Eufemio A, et al. Assessment of dosimetric and positioning accuracy of a magnetic resonance imaging-only solution for external beam radiotherapy of pelvic anatomy. Phys Imaging Radiat Oncol 2019;11:1–8. https://doi.org/10.1016/j.phro.2019.06.001.

[14] Korhonen J, Kapanen M, Sonke JJ, Wee L, Salli E, Keyrilainen J, et al. Feasibility of MRI-based reference images for image-guided radiotherapy of the pelvis with either cone-beam computed tomography or planar localization images. Acta Oncol 2015;54:889–95. https://doi.org/10.3109/0284186X.2014.958197.

[15] Tyagi N, Fontenla S, Zhang J, Cloutier M, Kadbi M, Mechalakos J, et al. Dosimetric and workflow evaluation of first commercial synthetic CT software for clinical use in pelvis. Phys Med Biol 2017;62:2961–75. https://doi.org/10.1088/1361-6560/aa5452.

[16] Masitho S, Szkitsak J, Grigo J, Fietkau R, Putz F, Bert C. Feasibility of artificial-intelligence-based synthetic computed tomography in a magnetic resonance-only radiotherapy workflow for brain radiotherapy: Two-way dose validation and 2D/2D kV-image-based positioning. Phys Imaging Radiat Oncol 2022;24:111–7. https://doi.org/10.1016/j.phro.2022.10.002.

[17] Bird D, Beasley M, Nix MG, Tyyger M, McCallum H, Teo M, et al. Patient position verification in magnetic-resonance imaging only radiotherapy of anal and rectal cancers. Phys Imaging Radiat Oncol 2021;19:72–7. https://doi.org/10.1016/j.phro.2021.07.005.

[18] Doemer A, Chetty IJ, Glide-Hurst C, Nurushev T, Hearshen D, Pantelic M, et al. Evaluating organ delineation, dose calculation and daily localization in an open-MRI simulation workflow for prostate cancer patients. Radiat Oncol 2015;10:37. https://doi.org/10.1186/s13014-014-0309-0.

[19] Wyatt JJ, Brooks RL, Ainslie D, Wilkins E, Raven E, Pilling K, et al. The accuracy of Magnetic Resonance – Cone Beam Computed Tomography soft-tissue matching for prostate radiotherapy. Phys Imaging Radiat Oncol 2019;12:49–55. https://doi.org/10.1016/j.phro.2019.11.005.

[20] Brooks RL, McCallum HM, Pearson RA, Pilling K, Wyatt J. Are cone beam CT image matching skills transferrable from planning CT to planning MRI for MR-only prostate radiotherapy? Br J Radiol 2021;94:20210146. https://doi.org/10.1259/bjr.20210146.

[21] McNair HA, Harris EJ, Hansen VN, Thomas K, South C, Hafeez S, et al. Magnitude of observer error using cone beam CT for prostate interfraction motion estimation: effect of reducing scan length or increasing exposure. Br J Radiol 2015;88:20150208. https://doi.org/10.1259/bjr.20150208.

[22] Parker RA, Scott C, Inacio V, Stevens NT. Using multiple agreement methods for continuous repeated measures data: a tutorial for practitioners. BMC Med Res Methodol 2020;20:154. https://doi.org/10.1186/s12874-020-01022-x.

[23] Wolf J, Nicholls J, Hunter P, Nguyen DT, Keall P, Martin J. Dosimetric impact of intrafraction rotations in stereotactic prostate radiotherapy: A subset analysis of the TROG 15.01 SPARK trial. Radiother Oncol 2019;136:143–7. https://doi.org/10.1016/j.radonc.2019.04.013.

[24] Edmund JM, Andreasen D, Van Leemput K. Cone beam computed tomography based image guidance and quality assessment of prostate cancer for magnetic resonance imaging-only radiotherapy in the pelvis. Phys Imaging Radiat Oncol 2021;18:55–60. https://doi.org/10.1016/j.phro.2021.05.001.